Chemical diffusion for CoO and Cu2O deduced from creep transitories

C. Clauss, A. Dominguez-Rodriguez, J. Castaing

Tome 21 N° 6 JUIN 1986

REVUE DE PHYSIQUE APPLIQUÉE

Revue Phys. Appl. **21** (1986) 343-348 JUIN **1986,** PAGE 343

Classification
Physics Abstracts
62.20 — 66.30

Chemical diffusion for CoO and Cu_2O deduced from creep transitories

C. Clauss, A. Dominguez-Rodriguez (*) and J. Castaing

Laboratoire de Physique des Matériaux, CNRS-Bellevue, 1, place Aristide Briand ,92195 Meudon Cedex, France

(*Reçu le 23 décembre 1985, accepté le 21 février 1986*)

Résumé. — A la suite d'un changement de pression d'oxygène, l'analyse du fluage transitoire nous a permis de déterminer un coefficient de diffusion chimique pour les monocristaux et polycristaux de CoO et Cu_2O. Le retour à l'équilibre de la concentration des défauts ponctuels se fait au même rythme pour tous les défauts concernés. Les joints de grains n'accélèrent pas ce processus de façon sensible.

Abstract. — The analysis of creep transitories after a change in oxygen partial pressure, allowed us to determine chemical diffusion coefficients for CoO and Cu_2O, single- and polycrystals. The rate of equilibration of point defect concentrations is similar for all defects. Grain boundaries do not seem to accelerate the process.

1. Introduction.

In binary oxides at thermodynamic equilibrium the concentrations of point defects, for a given pressure, are fixed by the temperature T and the oxygen activity, *viz.* the oxygen partial pressure P_{O_2} in the atmosphere surrounding the specimen. When changing T or P_{O_2}, new equilibrium conditions are reached *via* diffusion of point defects from (or to) the surface, where they are created (or annihilated). The diffusion takes place under chemical potential gradients, which correspond to chemical diffusion conditions [1]. It is rather easy to follow the changes with time of the concentration of point defects related to non stoichiometry by thermogravimetry or electrical conductivity; transitories have been analysed for $Co_{1-x}O$ and $Cu_{2-x}O$ giving a chemical diffusion coefficient [2-5] which is proportional to the cation vacancy V_{Co} or V_{Cu} diffusion coefficient. These defects are responsible for the departure from stoichiometry and their concentrations dominate those of all other types of defects. Cation vacancies are majority defects and the others are minority defects [6].

Information on minority defect structure is difficult to gather since they are in very low concentrations; selective properties are needed. Measurements of the slowest diffusing species is one of those and they can be achieved by the high temperature plastic deformation or creep. When deformation is controlled by the transport of matter [7], the creep rate $\dot{\varepsilon}$ is proportional to the oxygen self-diffusion coefficient in $Co_{1-x}O$ and $Cu_{2-x}O$ [6]. $\dot{\varepsilon}$ is then directly related to the concentration of minority point defects in the oxygen sublattice.

A creep transitory following a change of T or P_{O_2} is dominated by the rate of equilibrium of the minority defect concentration. In a previous study on CoO single crystal creep, the chemical diffusion coefficient $\tilde{D}_\varepsilon$ for minority defects has been found close to those determined for majority defects [8, 9]. However, the analysis was based on a mechanical model which was not appropriate and has been improved in the present work. In addition, we have extended the study in two directions : (i) CoO polycrystals have been used to look for an enhancement of the rate of equilibration due to short circuit diffusion; (ii) creep transitories have

(*) *Permanent address* : Dpto. Optica Universidad de Sevilla, 41080 Sevilla, Spain.

been performed in an other compound (Cu_2O) to check for the extent of the previous conclusions [8, 9].

2. Experimental techniques.

2.1 CREEP MEASUREMENTS. — Creeps tests have been performed on Cu_2O and CoO, single and polycrystals according to experimental techniques already used in previous works [10, 11]. We have restricted our experiments to the following conditions :

CoO : $1\,100 < T < 1\,400$ °C;

$P_{O_2} = 10^{-5}$ atm and 0.21 atm (air)

Cu_2O : $700 < T < 850$ °C;

$P_{O_2} = 5 \times 10^{-6}$ atm and 5×10^{-4} atm.

The applied stresses were chosen to provide the conditions where [7] :

$$\dot{\varepsilon} = K\sigma^n c \qquad (1)$$

c = minority point defect concentration

n = stress exponent

K is for the parameters of the creep equation which are not shown in equation (1).

Transitory creep, after P_{O_2} changes only, have been performed, by recording the length of the specimens under constant load and T. The analysis of the creep curves allows to plot log $\dot{\varepsilon}$ *versus* ε.

In this plot, when a specimen deforms homogeneously in compression under constant load, equation (1) gives a straigth line [7] which can be seen in figure 1 after the transitory.

Since we want to follow the rate of equilibration, the data are best represented as a function of time t. The linear relation log $\dot{\varepsilon} - \varepsilon$ is mathematically equivalent to a linear relation between $\dot{\varepsilon}^{-1}$ and t [8]. This is illustrated in figure 2.

The plots of figures 1 and 2 are equivalent for steady state; however, the extrapolated $\dot{\varepsilon}$ to the instant of the P_{O_2} change ($t_s = 0$) are different. This arises from the fact that the extrapolated $\dot{\varepsilon}$ depends on the extent of the transitory. The $\dot{\varepsilon}$ values at ε_s (Fig. 1) or $t_s = 0$ (Fig. 2) have, therefore, no physical meaning. The influence of P_{O_2} on steady state creep [10, 11] cannot be determined accurately from these tests (Figs. 1 and 2); it has to be studied when transients are not present or can be neglected.

2.2 EXPERIMENTAL ACCURACY AND LIMITATIONS. — Only P_{O_2} is changed at the initial time $t_s = 0$ of a creep transitory. This is achieved by flowing different gaz mixtures through the specimen chamber. We have used two different creep machines.

For Cu_2O, we have used a set-up described in [11, 12] where a pipe brings the gaz mixtures directly at the level of the specimen; the P_{O_2} change occurs very quickly after the introduction of a new gaz mixture.

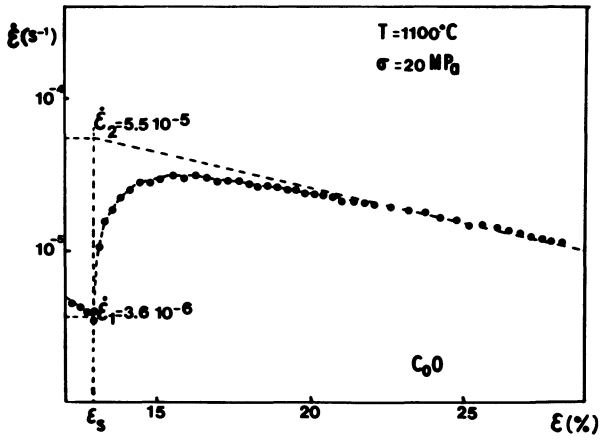

Fig. 1. — Transitory creep for CoO single crystal. The data are those of figure 4, reference [8] plotted as log $\dot{\varepsilon}$ *vs.* ε. The curve is linear for steady state reached at $\varepsilon > 23$ %.

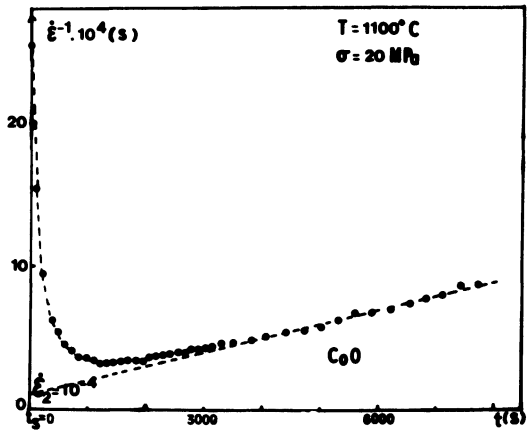

Fig. 2. — Same transitory as in figure 1 plotted as $1/\dot{\varepsilon}$ *vs.* time t. The curve is linear for $t > 4\,000$ s.

The temperature is held constant at a thermocouple close to the specimen. However, the introduction of a new gas mixture with a thermal conductivity different from the previous one, alters the temperature gradients in the chamber, thus inducing dilation recorded as specimen deformation. A change from argon to air with $\dot{\varepsilon} = 0$ gave an apparent specimen elongation of 45 μm in 2 hours at 850 °C.

This can induce an error, but did not happen in our Cu_2O experiments since we used flows of argon with 5 ppm and 500 ppm oxygen which have the same thermal properties.

The creep machine used for CoO is described in [13]; it showed a similar thermal behaviour. When flowing air instead of argon, a dilation corresponding to shortening the specimen by 9 μm occurred within 20 min, at 1 200 °C. We have estimated the error induced on a transitory creep and have shown that it could be neglected [14].

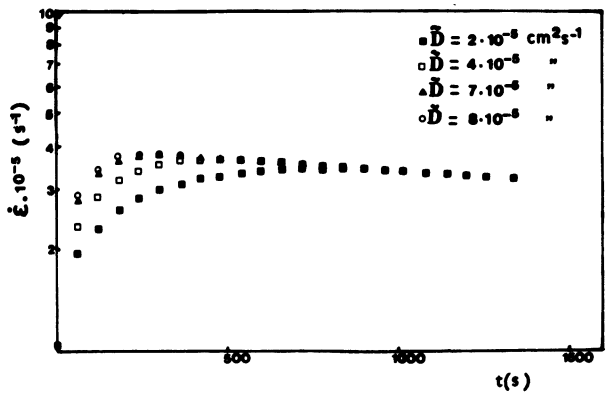

Fig. 3. — Calculated creep rates $\dot{\varepsilon}$ *vs.* time t using the model of section 2.3 for different D values.

There is an other limitation due to the speed of P_{O_2} change at the level of the CoO specimens. The gas is introduced at the bottom of the machine [13], and it takes some time to reach the specimens. We have measured this time by placing a zirconia cell at the specimen to follow the rate of the P_{O_2} change; it took about 300 s to reach $P_{O_2} = 0.21$ atm from 10^{-5} atm. This induced an experimental limitation to $\tilde{D}_\varepsilon$ values; for a specimen of 3 mm, $\tilde{D}_\varepsilon$ must be smaller than 3×10^{-5} cm²/s to correspond to a diffusion controlled mechanism. This condition was fulfilled in our experiments (see below, Fig. 4).

2.3 ANALYSIS OF CREEP TRANSITORIES. — We have analysed the transitories by assuming that the same creep equation (1) is valid at any time t. It corresponds to plastic deformation rate controlled by the diffusion of the slowest species [6, 7]. During the transitories,

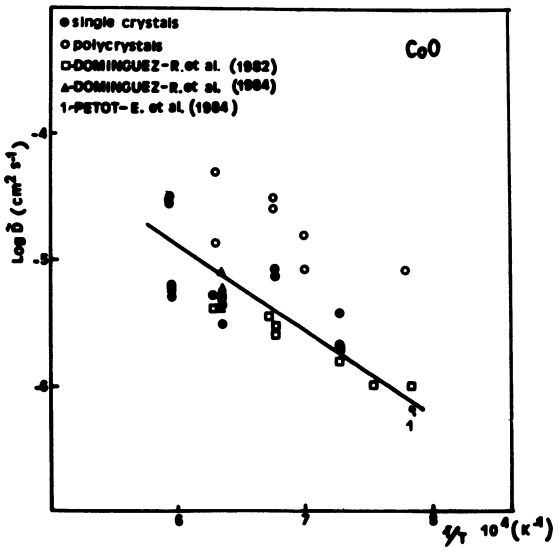

Fig. 4. — Arrhenius plot of the chemical diffusion coefficients $\tilde{D}$ for CoO. The points for single crystals are deduced from a reanalysis of data of [8] and [9]. For the line 1, $\tilde{D}$ was deduced from electrical conductivity [3].

the point defect concentrations at the surface are fixed by the new P_{O_2} and diffusion takes place from the lateral faces of the specimen, a parallelepiped of sizes X, Y, Z. We assume uniform concentrations along the Z direction which is parallel to the stress.

The concentration $C(x, y, t)$ of point defects in equation (1) can be calculated by solving the Fick's equation :

$$\frac{\partial^2 C}{\partial t^2} = D\left(\frac{\partial^2 C}{\partial x^2} + \frac{\partial^2 C}{\partial y^2}\right). \tag{2}$$

With the boundary conditions :

$$\begin{aligned} C &= C_1 \quad \text{at} \quad t < t_s = 0 \\ C &= C_2 \quad \text{at} \quad \begin{cases} t \geqslant t_s = 0 \\ x = 0 \text{ and } X \\ y = 0 \text{ and } Y . \end{cases} \end{aligned} \tag{3}$$

Following Crank [15], we can write :

$$C(x, y, t) = C_2 + \frac{16}{\pi^2}(C_1 - C_2)\, S(x, X, t, \tilde{D}) \times \times S(y, Y, t, \tilde{D}) \tag{4}$$

$$S(x, X, t, \tilde{D}) = \sum_{n=0}^{\infty} \frac{1}{2n+1} \sin \frac{(2n+1)\pi x}{X} \times \times \exp - \frac{(2n+1)^2 \pi^2 \tilde{D} t}{X^2} \tag{5}$$

and similar expression for $S(y, Y, t, \tilde{D})$.

We have now to express the mechanical coupling of the different parts of the specimen, which has a strength gradient induced by the point defect distribution $C(x, y, t)$, a scheme which is more appropriate than the one used previously [8, 9]. The compressive force F results in a heterogeneous stress $\sigma(x, y, t)$ under the condition of uniform strain rate $\dot{\varepsilon}(t)$. At any time t, one may write with equation (1) :

$$\dot{\varepsilon}(t) = K[\sigma(x, y, t)]^n\, C(x, y, t) \tag{6}$$

$\sigma(x, y, t)$ is unknown and needs not be calculated. It is related to F by :

$$F = \sigma XY = \int_0^X \int_0^Y \sigma(x, y, t)\, dx\, dy . \tag{7}$$

By calculating $\sigma(x, y, t)$ from equation (6) and introducing it into equation (7), one finds :

$$\dot{\varepsilon}(t) = K\sigma^n \frac{(XY)^n}{\left\{\int_0^x \int_0^y dx\, dy [C(x, y, t)]^{-1/n}\right\}^n} . \tag{8}$$

Equation (1) allows to write $C_1/C_2 = \dot{\varepsilon}_1/\dot{\varepsilon}_2$ at t_s. Equation (4) gives the transitory which is now describ-

ed by :

$$\dot{\varepsilon}(t) = (\alpha t + \dot{\varepsilon}_2^{-1})^{-1} \frac{(XY)^n}{\left\{ \int_0^x \int_0^y \mathrm{d}x\,\mathrm{d}y \left[1 + \frac{16}{\pi^2} \left(\frac{\dot{\varepsilon}_1}{\dot{\varepsilon}_2} - 1 \right) S(x, X, t, \tilde{D})\, S(y, Y, t, \tilde{D}) \right]^{-1/n} \right\}^n}. \quad (9)$$

We have written the creep behaviour at large time after the P_{O_2} change in the form [8] :

$$\dot{\varepsilon}^{-1} = \alpha t + \dot{\varepsilon}_2^{-1} \quad (10)$$

where α is the slope of the linear part of the curve (Fig. 2).

The only unknown in the equation (9) is $\tilde{D}$ which is adjusted in order to obtain the best fit with experimental data. The calculated transitories are very sensitive to the $\tilde{D}$ values (Fig. 3) and rather insensitive to n; the calculated transitories with $n = 1$ and $n = 5.2$ are as close as those corresponding to $\tilde{D} = 7 \times 10^{-5}$ and $\tilde{D} = 8 \times 10^{-5}$ cm^2/s in figure 3 [14].

The shape of the transitories are similar to those found in [8] although our analysis takes into account the actual conditions of deformation; it may be noted that for $n = 1$, our analysis is identical to the one used in [8]. Since the calculated transitories are hardly sensitive to n, it explains why the results found with both analysis for CoO single crystals are similar (see Sect. 3.1).

3. Experimental results.

3.1 CoO SINGLE CRYSTALS. — We have not performed any new creep test on CoO single crystals. We have analysed the transitories of Dominguez *et al.* [8, 9] (Figs. 1 and 2) using our model (see Sect. 2.3) to fit with experimental results. The $\tilde{D}$ values that we have found are plotted in figure 4; they are close to those already published. The disagreement between our analysis and the previous ones (Fig. 4) originates in the way the experimental data are evaluated, in particular the way to determine the beginning of the steady state after a transitory. Nevertheless, the conclusions of the previous work [8, 9] are unaltered.

3.2 CoO POLYCRYSTALS. — Creep tests have been performed on CoO polycrystals obtained by sintering of high purity powder identical to the one used in the preparation of single crystals [8-10]. The anneal was performed in the creep machine, directly before testing. This prevented the formation of Co_3O_4 which, usually, results in specimen failure when it decomposes to CoO.

Creep tests were started on porous materials which densified by deformation. Transitories at small deformation were so fast that they were controlled by the rate of P_{O_2} change in the gas mixture (see Sect. 2.2) instead of point defect diffusion. We have performed 16 transitories and retained only 10 of them (Fig. 4) that have been obtained for $\varepsilon \geqslant 30$-$40\,\%$. The fit between experiments and the model was made with X and Y equal to the size of the specimens; it is much larger than the grain size which is about 20 μm. $\tilde{D}$ values are shown in figure 4; they are larger than those for single crystals by less than a factor of 10, and are a little more scattered.

3.3 Cu_2O SINGLE AND POLYCRYSTALS. — Creep transitories have been studied for Cu_2O single crystals prepared as described in [11, 19]. The polycrystals were made by hot pressing [13, 20]; they contain a porosity between 5 and 10 %, and have grain sizes which can vary between 15 μm and 30 μm during a creep test [14]. The transitories are very fast; experiments had to be performed at low temperature and P_{O_2} (Fig. 5) in the creep machine first mentioned in section 2.2. The agreement between creep and calculated data was good (Fig. 5) for 11 transitories performed on single crystals and 6 on polycrystals. The corresponding $\tilde{D}$ are plotted in figure 6. In spite of their scatter, we can see that all data fall in the same decade for single and polycrystals as well as those deduced from electrical conductivity (Fig. 6). This result is similar to the one already displayed for CoO (Fig. 4).

4. Discussion.

4.1 CREEP TRANSITORIES. — A change in P_{O_2} may result in an increase of $\dot{\varepsilon}$ by a factor of 10 [10]. If it is performed without unloading, $\dot{\varepsilon}$ undergoes a transient

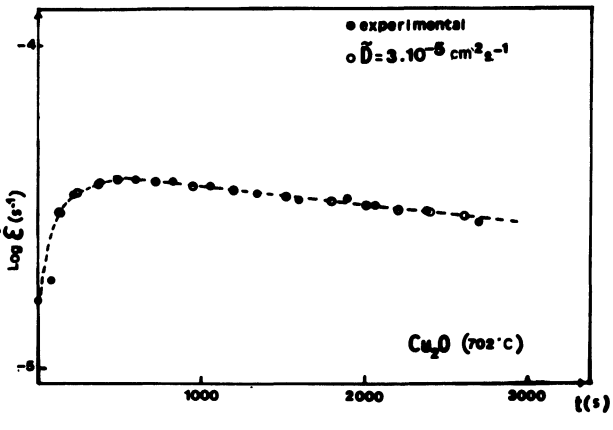

Fig. 5. — Transitory creep for Cu_2O single crystal showing a good agreement between experimental and calculated values.

(Figs. 1 and 5) that we have related to the evolution of point defect concentration through equation (1).

We have to examine the role of the microstructure which may be changed when $\dot{\varepsilon}$ is multiplied by 10. The most prominent feature of the creep microstructure is the polygonization [7, 16]. The cell size d is known to depend only on the stress σ [16]. If it varies after a P_{O_2} change, $\dot{\varepsilon}$ is affected. For $\dot{\varepsilon}$ multiplied by 10, we can expect that d is multiplied by $\sqrt{10}$ [16], which is not observed for CoO; after deformation at the same T and σ, under $P_{O_2} = 0.21$ atm and 10^{-5} atm, subgrain sizes of 70 μm and 60 μm, respectively, have been found, which were considered identical [17]. We have no evidence of any variation of d related to creep transitories. However, when $\dot{\varepsilon}$ is multiplied by 10, there must be some changes in the dislocation microstructure. Since the deformation is due to dislocation glide [7, 10, 11], the product dislocation density by mobility must be increased by a factor of 10. At high temperature, where there is no obstacle to glide, this should be a fast process compared to the length of the transitories. The creep-rate is therefore controlled by the climb of dislocations during transitories as well as during steady state. The use of equation (1), which is the base of our analysis, is then justified.

A chemical diffusion coefficient $\tilde{D}$ has been calculated. The results show a fairly large scatter (Figs. 4 and 6). A source of uncertainty comes from the $\dot{\varepsilon}$ fluctuations and from the difficulty to determine the beginning of steady state creep (see e.g. Fig. 1 in [8]). We believe that it is the origin of most of the scatter of $\tilde{D}$ values (Figs. 4 and 6).

4.2 CHEMICAL DIFFUSION. — We know that $\dot{\varepsilon}$ is directly related to minority point defects, viz defects in the oxygen sublattice for Cu_2O and CoO [10, 11, 20]. We therefore expect $\tilde{D}$ (Figs. 4 and 6) to characterize the kinetics of equilibration of oxygen vacancies or interstitials. For both Cu_2O and CoO, we find that $\tilde{D}$ values fall within an order of magnitude of $\tilde{D}$ deduced from majority point defect studies (Figs. 4 and 6). We do not believe that the difference between the two sets of values is meaningful. We conclude that the kinetics for equilibration of minority and majority point defects are identical. It is unlikely that this occurs by chance, because of a combination of different diffusion paths for the various defects in CoO [9] and Cu_2O. In particular, the creep microstructure does not seem to enhance the diffusion; this was checked in detail for CoO [9].

It is more surprising that grain boundaries are not even short circuits. They may enhance diffusion in CoO (Fig. 4) but not in Cu_2O (Fig. 6). If grain boundaries were perfect short circuits, they would be the place for creation or annihilation of point defects. Equilibration would take place by diffusion through the bulk of the grains which have sizes of 20 to 30 μm, i.e. the diffusion path would be 100 times shorter than for transport from the specimen surface. The time to reach equilibrium would therefore be 10^4 times shorter for polycrystals than for single crystals, which is not observed.

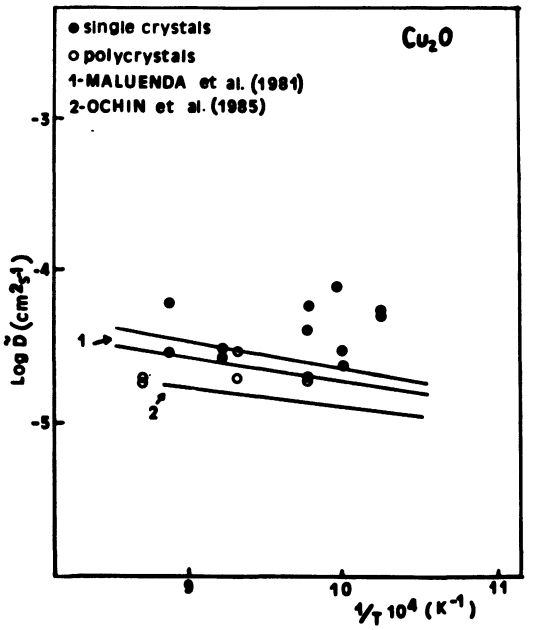

Fig. 6. — Arrhenius plot for chemical diffusion coefficients $\tilde{D}$ for Cu_2O. Results of Maluenda [4] and Ochin [5] are deduced from electrical conductivity.

The creep transitories in Cu_2O and CoO are directly related to the diffusion of cation vacancies, with negligible enhancement due to dislocations and grain boundaries. However, it has been found in NiO that Ni self-diffusion is enhanced by dislocations [18]. CoO and NiO have many similar properties which may include cation diffusion enhancement. During plastic deformation, the dislocation density has to be, at least, as high as the one in Atkinson's experiments on NiO [18]. Dislocations enhance the cation self-diffusion but not the cation vacancy diffusion. This is an indication that the enhancement is due to an increase in point defect concentrations, not in their mobility.

Acknowledgments.

The authors are indebted to B. Pellissier for his technical assistance in the creep tests.

References

[1] KOFSTAD, P., *Non stoichiometry, diffusion and electrical conductivity in binary metal oxides,* 1972 ed.

[2] WIMMER, J. M., BLUMENTHAL, R. N., BRANSKY, I., *J. Phys. Chem. Solids* **36** (1972) 269.

[3] PETOT-ERVAS, G., RADJI, O., SOSSA, B., OCHIN, P., *Rad. Eff.* **75** (1983) 301.

[4] MALUENDA, J., FARHI, R., PETOT-ERVAS, G., *J. Phys. Chem. Solids* **42** (1981) 697.

[5] OCHIN, P., PETOT-ERVAS, G. and PETOT, C., *J. Phys. Chem. Solids* **46** (1985) 695.

[6] MONTY, C., *Défauts ponctuels dans les solides*, Ecole d'Eté de Confolant (Editions de Physique) 1978.

[7] BRETHEAU, T., CASTAING, J., RABIER, J. and VEYSSIÈRE, P., *Adv. Phys.* **28** (1979) 829.

[8] DOMINGUEZ-RODRIGUEZ, A., MONTY, C. and PHILIBERT, J., *Philos. Mag.* **A 46** (1982) 869.

[9] DOMINGUEZ-RODRIGUEZ, A., MONTY, C., CASTAING, J. and PHILIBERT, J., *Solid State Ionics* **12** (1984) 353.

[10] DOMINGUEZ-RODRIGUEZ, A., SANCHEZ, M., MARQUEZ, R., CASTAING, J., MONTY, C., PHILIBERT, J., *Philos. Mag.* **A 46** (1982) 411.

[11] BRETHEAU, T., MARHIC, C., SPENDEL, M. and CASTAING, J., *Philos. Mag.* **35** (1977) 1473.

[12] POIRIER, J. P., *Philos. Mag.* **26** (1972) 701.

[13] GERVAIS, H., PELLISSIER, B., CASTAING, J., *Rev. Int. Hautes Temp. Refract.* **15** (1978) 43.

[14] CLAUSS, C., Thèse 3e cycle, Paris VI (1984).

[15] CRANK, J., *The mathematics of diffusion,* Second edition (Clarendon Press, Oxford) 1967.

[16] POIRIER, J. P., *Creep of crystals* (Cambridge University Press) 1985.

[17] CASTAING, J., DOMINGUEZ-RODRIGUEZ, A., *Int. Conf. on Defects in Insulating Crystals,* Salt Lake City (1983), Abstract book p. 78-79.

[18] ATKINSON, A., TAYLOR, R. I., *Philos. Mag.* **39** (1979) 581.

[19] AUDOUARD, A., CASTAING, J., RIVIÈRE, J. P. and SIEBER, B., *Acta Met.* **29** (1981) 1385.

[20] BRETHEAU, T., PELLISSIER, B. and SIEBER, B., *Acta Met.* **29** (1981) 1617.